

SCIENTIFIC REPORTS

OPEN

Large-Scale Production of Large-Size Atomically Thin Semiconducting Molybdenum Dichalcogenide Sheets in Water and Its Application for Supercapacitor

Received: 05 February 2016

Accepted: 03 May 2016

Published: 26 May 2016

Yu-Xiang Chen¹, Chien-Wei Wu², Ting-Yang Kuo², Yu-Lung Chang¹, Ming-Hsing Jen¹ & I-Wen Peter Chen¹

To progress from laboratory research to commercial applications, it is necessary to develop an effective method to prepare large quantities and high-quality of the large-size atomically thin molybdenum dichalcogenides (MoS_2). Aqueous-phase processes provide a viable method for producing thin MoS_2 sheets using organolithium-assisted exfoliation; unfortunately, this method is hindered by changing pristine semiconducting 2H phase to distorted metallic 1T phase. Recovery of the intrinsic 2H phase typically involves heating of the 1T MoS_2 sheets on solid substrates at high temperature. This has restricted and hindered the utilization of 2H phase MoS_2 sheets suspensions. Here, we demonstrate that the synergistic effect of the rigid planar structure and charged nature of organic salt such as imidazole (ImH) can be successfully used to produce atomically thin 2H- MoS_2 sheets suspension in water. Moreover, lateral size and area of the exfoliated sheet can be up to $50\ \mu\text{m}$ and $1000\ \mu\text{m}^2$, respectively. According to the XPS measurements, nearly 100% of the 2H- MoS_2 sheets was successfully prepared. A composite paper supercapacitor using the exfoliated 2H- MoS_2 and carbon nanotubes delivered a superior volumetric capacitance of $\sim 410\ \text{F}/\text{cm}^3$. Therefore, the organic salts-assisted liquid-phase exfoliation has great potential for large-scale production of 2H- MoS_2 suspensions for supercapacitor application.

Layered two-dimensional (2D) materials have drawn tremendous attention after Geim and Novosolov demonstrated that adhesive tape could be utilized to mechanically exfoliate graphite into one-atom-thick layers that can be used in atomically thin electronic devices¹. Graphene is the most well-known 2D nano-material owing to its superior physical, chemical and mechanical properties, though it has a zero bandgap which restricts its application in energy storage and low-power electronics². Structurally similar to graphene, the lamellar structure of transition metal dichalcogenides (TMDs) includes planes where the atoms of the transition metal and sulfur are covalently bonded and the nearby planes stack upon each other via a weak coupling interaction³. Due to their promising electronic and chemical properties, TMDs have attracted considerable attention in research as 2D layered materials. Recently, there has been a focus on atomically thin TMD preparations, most notably molybdenum dichalcogenides (MoS_2), because they are expected to show superior capacitive properties, which allows for potential applications in electronic devices^{4,5}. However, the lack of an effective exfoliation method for the large-scale production of high-concentration atomically thin 2H- MoS_2 sheets has been one of the obstacles to studying their chemical and physical properties and to using them for novel and practical applications.

Owing to high production prices and limited scalability, mechanical exfoliation limits the use of 2H- MoS_2 materials to fundamental research and special applications⁶. Similarly, the chemical vapor deposition method may be an alternative route for the scalable production of 2H- MoS_2 materials. However, it is not only hard to precisely control the stoichiometry ratio, but this method also involves high prices and rather low yields⁶. In contrast,

¹Department of Applied Science, National Taitung University, 369, Sec. 2, University Rd., Taitung City 95092, Taiwan. ²Department of Chemistry, National Taiwan University, 1, Sec. 4, Roosevelt Road, Taipei, 10617, Taiwan. Correspondence and requests for materials should be addressed to I.-W.P.C. (email: iwchen@nttu.edu.tw)

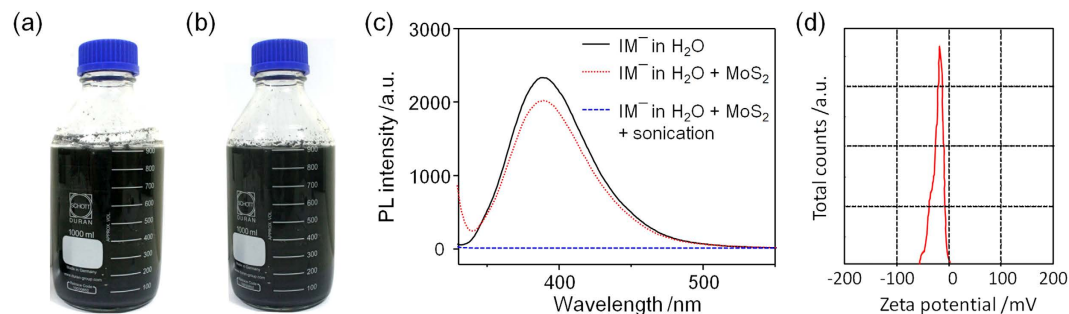


Figure 1. Large-scale production of 2H-MoS₂ sheets by ultrasonication. (a) An Im⁻-assisted exfoliated 2H-MoS₂ suspension on the liter-scale made by ultrasonic exfoliation. (b) The as-prepared 2H-MoS₂ suspension after standing for more than a year. (c) The PL spectra of Im⁻ (black line), Im⁻/2H-MoS₂ without sonication (red dotted line) and Im⁻/2H-MoS₂ with sonication (blue dashed line). (d) Zeta potential distributions of the Im⁻-assisted 2H-MoS₂ suspension.

the liquid phase exfoliation method is characterized by high scalability and relatively low production costs, and it does not require transfer techniques, thus making it suitable for producing 2H-MoS₂ materials in bulk quantities^{6,7}. Recently, liquid-phase routes have been demonstrated by sonicating MoS₂ powder in properly chosen solvents such as a mixture of ethanol and water or dimethylformamide and N-methylpyrrolidone, which can directly exfoliate MoS₂ powder and disperse the exfoliated MoS₂ sheets owing to their compatible surface energies^{8–10}. Coleman *et al.* have demonstrated that liquid-phase exfoliation of MoS₂ powder in N-methylpyrrolidone with ultrasonication is a practical route to achieving the preparation of MoS₂ sheets. However, this method yields multi-layered sheets of MoS₂, and thin sheets are very rarely observed^{10,11}. Recently, large amounts of multi-layered MoS₂ suspension were successfully prepared after more than 100 hours of sonication¹⁰ or several hours of grinding¹². This, however, provided exfoliated MoS₂ nanosheets less than 100 nm in size and affected its unique and original properties. Moreover, N-methylpyrrolidone is expensive and requires special attention while handling¹³. Unfortunately, one of the most ideal dispersion media, water, has a non-compatible surface energy that is too high to have an effect on its own for MoS₂ exfoliation. The best-known group of exfoliants involves electron donors, for example, organolithium compounds^{14–18}. Bulk MoS₂ can be exfoliated with lithium (Li) under rigorous conditions for more than 72 hours to obtain reduced Li_xMoS₂ with an expanded structure; this can be further exfoliated by a sonication-assisted process^{16,17}. However, Li-assisted exfoliation leads to a structural change in MoS₂ from the thermodynamically stable semiconducting 2H phase to the metastable metallic 1T phase^{16,17}. Moreover, 1T-MoS₂ turns into nanometer-sized flakes after exfoliation along with the occurrence of metal nanoparticle formation and Li₂S agglomeration¹⁹. This has dramatically hindered the development of atomically thin MoS₂ sheets in most applications that require a pristine structure and large sheets with high concentrations. Recently, an electrochemical method was successfully established to produce MoS₂ sheets. Nevertheless, mass production through this process is limited because Mo⁵⁺ and Mo⁶⁺ are generated^{20,21}. Exploration has recently been further extended to produce exfoliated MoS₂ sheets by the use of exfoliants in water or polymers in tetrahydrofuran^{22,23}. Polymer-assisted exfoliation methods in an aqueous solution with high-power probe sonication were reported, but the final concentration of less than 0.5 mg/mL and resulting small sheets were still far from the demands of practical applications requiring large quantities²². Inspired by the liquid phase exfoliation of graphene^{24–26}, a method with similar exfoliation principles may be an approach to boost the production of atomically thin 2H-MoS₂ sheets.

This study demonstrates that atomically thin MoS₂ sheets in the 2H phase can be prepared by organic salts such as imidazole (ImH) or pyridiniumtribromide (PyBr₃). The exfoliated 2H-MoS₂ sheet dimensions can be as large as to 1000 μm². In addition, nearly 100% of the composition was of the thermodynamically stable 2H phase structure. These exfoliants are cheap and commercially available, and the method can be performed under ambient conditions. Moreover, the 2H-MoS₂ suspension allows for the preparation of high electrical conductive composites for energy storage applications.

Results and Discussion

Figure S1a shows a photograph of the experimental setup for the ultrasonication exfoliation of 2H-MoS₂ powder (Fig. S1b). A suspension of the exfoliated 2H-MoS₂ sheets was prepared from commercial 2H-MoS₂ powder via an ImH or PyBr₃ exfoliation process followed by ultrasonication. Figure 1a shows that liter-scale 2H-MoS₂ suspensions can be prepared through Im⁻-assisted exfoliation. These highly-dispersed suspensions of 2H-MoS₂ sheets can stand for more than a year, and the suspension remained dark green in color, as shown in Fig. 1b. To unveil the exfoliation mechanism of the layered 2H-MoS₂, we performed a photoluminescence (PL) experiment. First, the Im⁻ solution showed PL emission at 388 nm (Fig. 1c; black solid line) under irradiation at 270 nm. Then, the MoS₂ powder was added to the Im⁻ solution. After shaking the mixture, the 2H-MoS₂/Im⁻ solution was left on the bench for 30 minutes (Fig. 1c; red dotted line). The PL intensity of the 2H-MoS₂/Im⁻ solution decreased, indicating that Im⁻ molecules, nearly one atom in thickness, adsorbed to the layered 2H-MoS₂. Finally, the MoS₂ powder was exfoliated by ultrasonication to generate large quantities of the atomically thin 2H-MoS₂ sheets in suspension. Interestingly, the PL intensity of 2H-MoS₂/Im⁻ was fully quenched (Fig. 1c; blue line), which demonstrates that nearly all of the Im⁻ molecules adsorbed to the exfoliated 2H-MoS₂ surfaces. The zeta

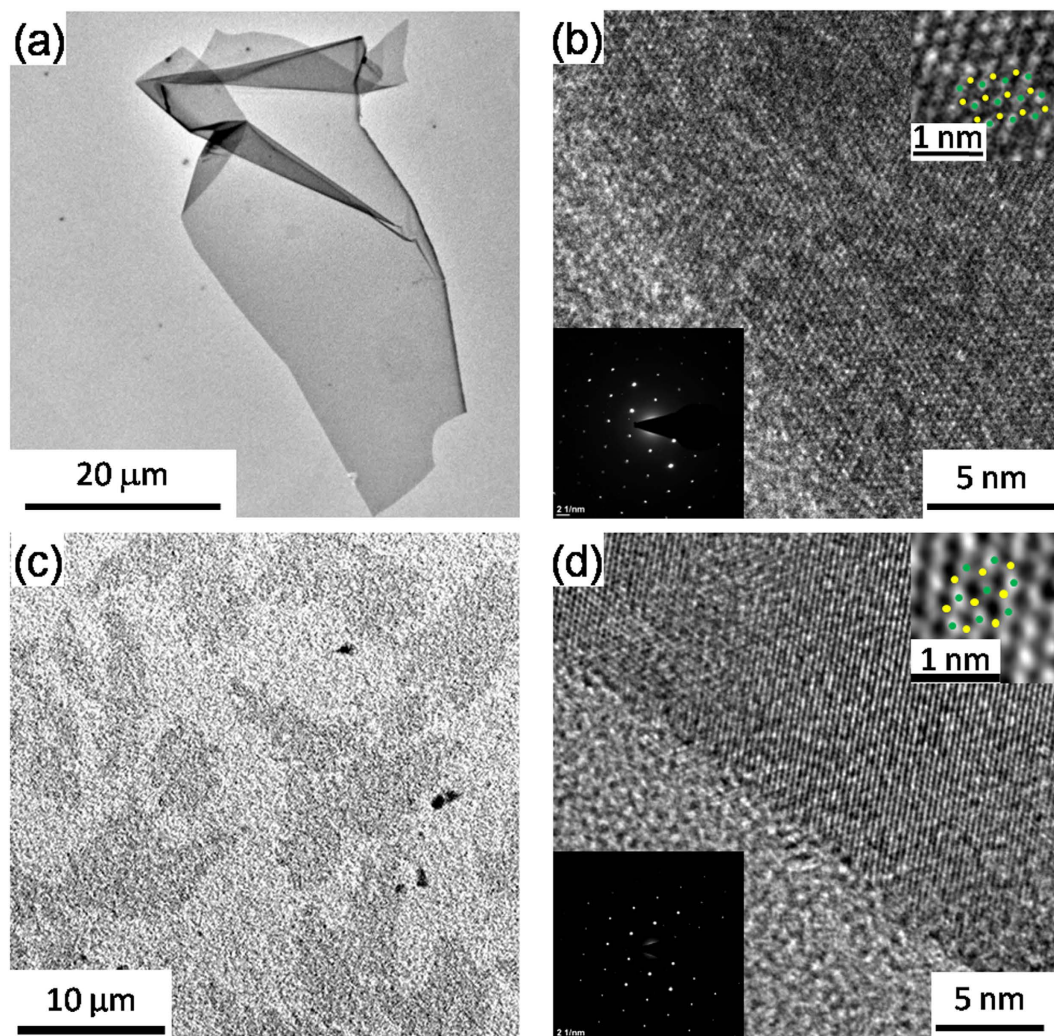


Figure 2. Morphological characterization of the exfoliated 2H-MoS₂ sheets. (a,c) TEM images of Py⁺-assisted and Im⁻-assisted exfoliated 2H-MoS₂ sheets, respectively. (b,d) HRTEM images of Py⁺-assisted and Im⁻-assisted exfoliated 2H-MoS₂ sheets, respectively. The bottom insets of (b,d) show the selected area electron diffraction (SAED) pattern of the Py⁺-assisted and Im⁻-assisted exfoliated 2H-MoS₂ sheets, respectively. Upper insets show individual Mo (green dot) and S (yellow dot) atoms and their honeycomb arrangement.

potential of the suspension of the exfoliated 2H-MoS₂ sheets was -22.4 mV (Fig. 1d), which demonstrated its superior aqueous stability with the assistance of Im⁻ molecules. The negative surface charges provide evidence of electrostatic repulsion forces between each of the exfoliated 2H-MoS₂ sheets, resulting in a stable aqueous suspension. In the X-ray diffraction (XRD) patterns, the intensity of the (002) reflection of the exfoliated 2H-MoS₂ is significantly weaker than the bulk MoS₂ powder, which means that a large amount of the exfoliated 2H-MoS₂ thin sheets prepared were highly exfoliated (Fig. S2)^{21,27-29}. Just as reported in the literature, the planar structure of the MoS₂ flakes was hydrophobic^{30,31}. Meanwhile, the ring of the Im⁻ molecules also possesses a hydrophobic property³². Therefore, the mechanism for the Im⁻-assisted exfoliation of layered 2H-MoS₂ materials is attributed to hydrophobic-hydrophobic interaction. The exfoliated 2H-MoS₂ flakes are stabilized due to the electrostatic repulsive forces generated by the planar charged organic molecules.

Figures 2a,c show transmission electron microscopy (TEM) images of a thin 2H-MoS₂ sheet. Figure S3 shows large flakes of the exfoliated 2H-MoS₂. The exfoliated 2H-MoS₂ sheets are characterized through the edge of the sheets which shows that large-area 2H-MoS₂ flakes are mostly all monolayer via the high resolution TEM (HRTEM) images as shown in the inset of Fig. S3. The exfoliated 2H-MoS₂ sheets had a maximum lateral size of over $50\ \mu\text{m}$, which is nearly two orders of magnitude larger than using exfoliant-assisted methods^{16,17} or the solvent exfoliated method^{11,12}. Intriguingly, the production of thin 2H-MoS₂ sheets with an unprecedented sheet size of up to $1000\ \mu\text{m}^2$ was achievable (Fig. 2a). The HRTEM images in Fig. 2b,d show that the lattice structure of the edge of the exfoliated 2H-MoS₂ sheet was not damaged during the ultrasonic exfoliation process. In addition, the diffraction patterns of the insets in Fig. 2b,d show lattice spacing of 0.2764 and 0.2797 nm, respectively; both match the (100) plane of typical 2H-MoS₂ sheets³³. On the basis of the above results, the synergistic effect of the charged nature and the planar structure of the Im⁻ and Py⁺ enabled both the exfoliation of 2H-MoS₂ and

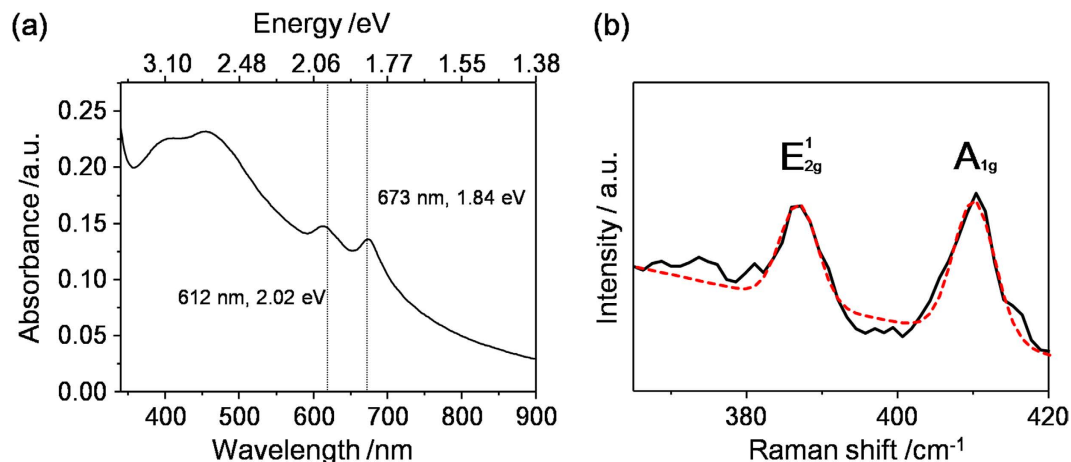


Figure 3. (a) UV-vis absorption and (b) Typical Raman spectrum of Im^- -assisted exfoliated 2H-MoS₂ sheets. (black line: experimental data; red dotted line: fitted peaks).

the stabilization of the 2H-MoS₂ suspension. Besides that, atomic force microscopy (AFM) is a powerful tool used in assessing the thickness of exfoliated 2H-MoS₂ sheets, which in turn correlates to the number of layers. The average thickness of 743 measured sheets from the substrate to the sheet was found to be ~ 0.9 nm, as shown in Fig. S4a. This statistical thickness is in good agreement with the reported 2H-MoS₂ monolayer thickness of $0.9 \sim 1.2$ nm^{11,16}. Figure S4b indicates that the flake size of most of the exfoliated 2H-MoS₂ sheets ranged from a few square micrometers to one thousand square micrometers. Based on the results of the PL, zeta potential, XRD, TEM and AFM measurements, a proposed schematic illustration of 2H-MoS₂ exfoliation is shown in Fig. S5.

Further structural characterization of the already-prepared concentration of the exfoliated 2H-MoS₂ sheets (1 mL) was diluted with about 400 mL of water and used to evaluate the absorption spectrum of the 2H-MoS₂ sample, as shown in Fig. 3a. The peaks centered at 400, 451, 612 and 673 nm were the representative absorption bands of the exfoliated 2H-MoS₂ in solution. The peaks at 400 and 451 nm could be ascribed to the direct transition from the valence band to the conduction band. The excitonic peaks at 612 and 673 nm, responsible for the K point of the Brillouin zone, were also clearly observed. These two characteristic peaks demonstrate the existence of high-quality atomically thin 2H-MoS₂ sheets. By utilizing Beer's law and the extinction coefficient centered at 672 nm $\alpha_{672} = 3400 \text{ mL}/(\text{mg}\cdot\text{m})$ ^{11,34}, we can estimate the concentration of the exfoliated MoS₂ sheets was ~ 2 mg/mL in our supernatant. However, the extinction coefficient may change with the solvent, so the value of 2 mg/mL should be considered a rough estimate³⁴. To obtain a more accurate concentration, we filtrated the already-prepared 2H-MoS₂ suspension. Then, it was dried at 200 °C for 2 h to remove the physisorbed exfoliant of Im^- . The concentration of the exfoliated 2H-MoS₂ suspension was ~ 4 mg/mL. The Im^- -assisted exfoliated 2H-MoS₂ sheets exhibited two Raman characteristic peaks at around 387 and 409 cm⁻¹ with full-width-half-maximum (FWHM) values of 3.6 and 6.8 cm⁻¹, corresponding to the E_{2g} and A_{1g} modes, respectively, as shown in Fig. 3b. Note that the Raman frequency difference between E_{2g} and A_{1g} is consistent with that of chemically exfoliated single-layer MoS₂³⁵. The ratio (E_{2g}/A_{1g}) of the integrated intensity of the Im^- -assisted exfoliated 2H-MoS₂ sheets was 0.59. Moreover, Fig. S6 shows that the Py⁺-assisted exfoliated 2H-MoS₂ also showed two Raman characteristic peaks with FWHM values of 6.2 and 4.4 cm⁻¹, corresponding to A_{1g} and E_{2g} modes, respectively. The ratio (E_{2g}/A_{1g}) of the integrated intensity of the Py⁺-assisted exfoliated MoS₂ sheet was 0.47. The peak FWHM values and the integrated intensity ratios were similar to those reported after mechanical exfoliation of single-layer 2H-MoS₂ sheets, demonstrating the successful preparation of single-layer 2H-MoS₂ sheets³⁶.

We employed thermogravimetric analysis (TGA) to explore the thermal stability of the exfoliated 2H-MoS₂ sample. Figure 4a shows the TGA profile of the Im^- -assisted exfoliated 2H-MoS₂ sheets. The TGA curve of the exfoliated 2H-MoS₂ sheets shows one weight loss stage around 160 °C. The weight loss region with about 12% loss of the original weight which occurred around 110–190 °C was due to the decomposition of the adsorbed imidazolium molecules. After 200 °C, no further weight loss occurred. The differential TGA curve showed the Im^- -assisted exfoliated MoS₂ sheets had one major peak at 167 °C, which is consistent with the decomposition temperature of pure imidazole (Fig. S7). The TGA result demonstrates that there was no detectable oxidation in the exfoliated 2H-MoS₂ sheets. This confirmed that the production process did not result in the formation of S–O derivatives on the exfoliated 2H-MoS₂ sheets. According to previous studies, the thermodynamically stable 2H phase of MoS₂ is the trigonal prismatic phase where every molybdenum atom is coordinated by six neighboring sulfur atoms¹⁶. However, the MoS₂ structure could form a metastable phase where the coordination of Mo atoms becomes octahedral (1T-MoS₂) upon organolithium-assisted exfoliation^{14,16,17,37}. Therefore, we studied the phase composition of the exfoliated MoS₂ sheets with X-ray photoelectron spectroscopy (XPS). The Mo 3d of the XPS spectrum is shown in Fig. 4b. The Mo 3d spectrum shows peaks centered at 229.1 and 232.3 eV, corresponding to the Mo⁴⁺ 3d_{5/2} and Mo⁴⁺ 3d_{3/2} components of 2H-MoS₂, respectively. In addition, the spectrum shows two unobservable peaks at 228.3 and 231.4 eV, corresponding to the Mo⁴⁺ 3d_{5/2} and Mo⁴⁺ 3d_{3/2} components of

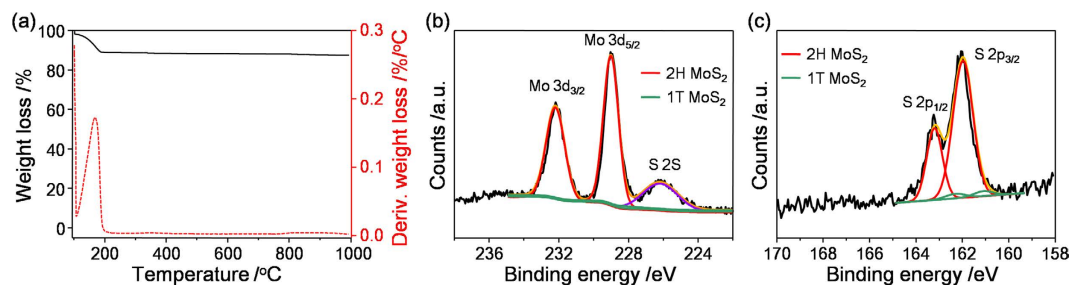


Figure 4. (a) TGA test of the exfoliated 2H-MoS₂ sheets (black line); differential weight loss (%/dT, red dashed lines) is shown as a function of temperature. (b) XPS spectrum showing the peak regions of Mo 3d and S 2s core level for the exfoliated 2H-MoS₂ sheets. (c) S 2p core level of the XPS spectrum for the exfoliated 2H-MoS₂ sheets. The samples were calibrated using the Au 4f_{5/2} line at 84.0 eV as a reference. After Shirley background subtraction, the peaks were fitted with Gaussian curve fitting. The Mo 3d and S 2p were deconvoluted to exhibit the 2H and 1T contributions, shown as red and green lines, respectively.

1T-MoS₂, respectively. Similarly, in the S 2p core level spectrum, Fig. 4c shows that two peaks were observed at 162.0 and 163.3 eV, corresponding to the S 2p_{3/2} and S 2p_{1/2} components of 2H-MoS₂, respectively. Additionally, the spectrum shows two weak peaks at 161.1 and 162.4 eV, corresponding to the S 2p_{3/2} and S 2p_{1/2} components of 1T-MoS₂, respectively. Moreover, no signals were detected in the range of 166 to 170 eV, indicating that sulfur elements also persisted in non-oxidized form. These results are in agreement with reported studies on MoS₂ single crystals, showing that the exfoliated MoS₂ sheets are predominantly in the 2H phase¹⁶. The exfoliated MoS₂ sheets contain over 95% of the 2H phase after exfoliant-assisted exfoliation. The remaining less than 5% of the non-2H phase was nearly fully converted to the 2H phase after annealing at 200 °C (Fig. S8). This exfoliation method demonstrates that exfoliated 2H-MoS₂ sheets preserve their thermodynamically stable semiconducting properties. This is in contrast to Li exfoliated MoS₂ in which the semiconducting properties of the sheets are perturbed due to their phase structural changes from the 2H to 1T phase. In addition, it is worth mentioning that the peak at 236 eV did not show a significant signal, attributed to Mo⁶⁺ 3d_{5/2}, indicating that the oxidized form of Mo⁶⁺ is difficult to detect. This result is superior to that of electrochemically exfoliated MoS₂ sheets that oxidize the pristine charge of Mo⁴⁺ to Mo⁵⁺ and Mo⁶⁺²¹.

The versatility of the exfoliation method allowed us to fabricate composite papers by directly adding dispersed carbon nanotubes (CNTs) to the 2H-MoS₂ suspension. Free-standing 2H-MoS₂/CNTs papers were peeled off from the filtered membrane, as shown in Fig. 5a. Scanning electron micrographs (SEM) of the 2H-MoS₂/CNTs paper at low (Fig. 5b) and high (Fig. 5c) magnification clearly showed that the 2H-MoS₂ sheets were wrapped in CNTs. To clearly understand the distribution of the 2H-MoS₂ sheets in the 2H-MoS₂/CNTs paper, Fig. 5d shows the mapping image from Raman spectroscopy of the composite paper by extracting the frequency of the characteristic peak of E_{2g}¹. The information in the Raman mapping spectrum shows similar Raman intensity of E_{2g}¹, which indicates a uniform dispersion of the 2H-MoS₂ in the composite paper. To compare the electrical conductivity of the composite papers, we compared a pure MoS₂ crystal with the composite papers. The addition of CNTs increased the electrical conductivity, σ , from $\sim 10^{-6}$ S/cm for the 2H-MoS₂ only film to $\sim 6 \times 10^2$ S/cm for the 2H-MoS₂/CNTs composite paper. The electrical conductivity of the 2H-MoS₂/CNTs hybrid paper compares superiorly with some of the other 2D materials' electrodes for supercapacitors³⁸. The capacitance of the 2H-MoS₂/CNTs hybrid paper was obtained using cyclic voltammetry (CV). The resulting CVs for potential ranged from 0 to 0.8 V versus NHE, as shown in Fig. S9a. The galvanostatic charging/discharging curves for the 2H-MoS₂/CNTs paper were recorded at different current densities as depicted in Fig. S9b. Figure S9c shows the volumetric capacitances at various current densities of supercapacitors based on 2H-MoS₂/CNT composite papers. The volumetric capacitance of the 2H-MoS₂/CNT hybridized supercapacitor was ~ 410 F/cm³ at a current density of 2 A/cm³. This value is superior to that of a film-based supercapacitor consisting of ZnO/graphene film (0.36 F/cm³)³⁹ MoS₂/CNTs (0.7 F/cm³)⁴⁰, MoS₂/reduced graphene oxide/CNTs (5.2 F/cm³)⁴⁰, and reduced graphene oxide/MoS₂ (30 F/cm³)⁴¹. Moreover, it is higher than the value of the best micro-supercapacitor based on carbide-derived carbon film⁴². The improved performance of the 2H-MoS₂/CNTs paper electrodes could be possibly attributed to three reasons. First, the Mo atoms of the exfoliated 2H-MoS₂ sheets possess many oxidation states from +2 to +6, promising a representative pseudo-capacitance behavior with high specific capacitance for 2H-MoS₂/CNTs hybrid paper⁴³. Second, the interconnected high conducting CNTs network provides electric double-layer capacitance and also serves as a conductive material for charge transport and transfer^{42,43}. Finally, the dispersed CNTs of the 2H-MoS₂/CNTs composite paper serve as spacers to mitigate restacking between the exfoliated 2H-MoS₂ sheets^{44,45}. The cyclic stability of the 2H-MoS₂/CNTs hybrid paper electrodes in a 0.5 M K₂SO₄ electrolyte was tested over 2,300 cycles (Fig. S9d) and maintained a capacitance in excess of 95% after 2,300 cycles.

Conclusion

We have demonstrated a universal route to the large-scale production of a high-concentration of large, atomically thin 2H-MoS₂ sheets that can be made by adding an organic salt. The lateral size and area of the exfoliated 2H-MoS₂ can reach 50 μ m and 1000 μ m², respectively, which is nearly two orders of magnitude greater than that of mechanically, Li-assisted chemically exfoliated MoS₂ sheets. The spectral analysis, which incorporated TEM, AFM, XRD, UV-vis, PL, Raman, XPS and TGA measurements, confirmed that the exfoliated MoS₂ sheets

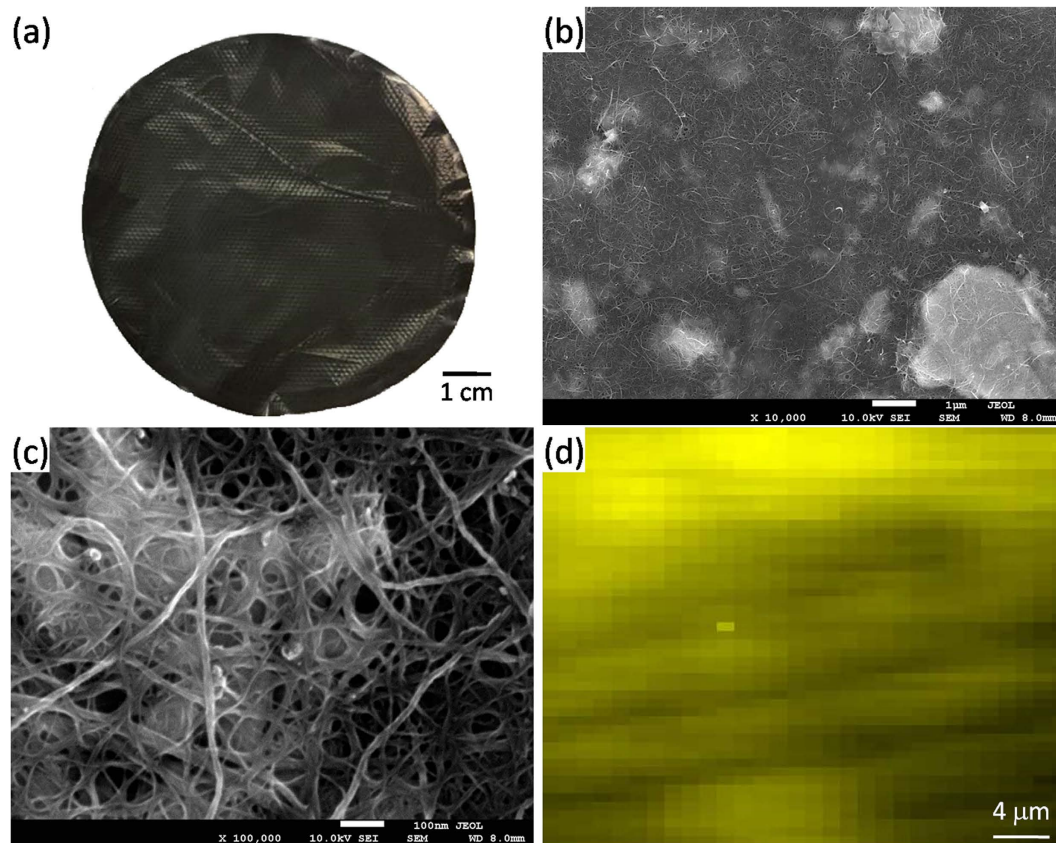


Figure 5. 2H-MoS₂/CNTs composite paper. (a) Photograph of the free-standing hybrid paper of 2H-MoS₂/CNTs. (b) low and (c) high magnification of FE-SEM images of the 2H-MoS₂/CNTs hybrid paper. (d) Raman image of the hybridized paper by extracting the frequency of the characteristic peak of E_{12g}. The Raman 2D mapping area is 40 × 60 μm.

predominately exhibited the 2H phase. We anticipate that fast progress in areas like hybrid paper processing and electronic device fabrication involving large-scale production of high-concentration, large, atomically thin 2H-MoS₂ sheets will develop from these results.

Methods

Materials. Molybdenum (IV) sulfide (99% metals basis; ~325 mesh powder) were purchased from Alfa Aesar. Imidazole (99%, ACROS) and pyridinium tribromide (TCI) were used without further purification as the exfoliant. Considering large-scale production of the 2H-MoS₂ suspension and the high cost, ImH is preferred. Single-walled carbon nanotubes powder (CG300-L16) were produced by SouthWest NanoTechnologies Inc. Multi-walled carbon nanotubes powder and Triton X-100 utilized in this study were produced by Golden Innovation Business Co. Ltd.

Exfoliation of MoS₂ powder. To exfoliate MoS₂ powder to form 2H-MoS₂ suspension, a high concentration of exfoliated 2H-MoS₂ sheets was prepared by using a Chromtech model UP-500 ultrasonic homogenizer with a ½-inch ultrasonic tip. 10 g of the MoS₂ powder, 20 g of imidazole and 1000 mL of deionized water (Elga Ltd., HighWycombe, Bucks, UK) was added to a 1000 mL beaker and sonicated with tip sonication (100 ~ 500 W) in continuous mode for 2 h. The exfoliation process was performed under an N₂ environment at controlled temperature of 15 °C (CC-1010, Panchun Sci. Corp.).

Preparation of 2H-MoS₂/CNT composite papers. The 108 mg CNT was sonicated in a water bath with the assistance of aqueous Triton X-100 dispersant for 1 h to achieve the CNT suspension of 1 L. Then was poured CNT dispersion of 250 mL and the Im⁻-assisted exfoliated as-exfoliated 2H-MoS₂ nanosheets suspension of 50 mL into the beaker. The mixture was sonicated with tip sonication (100 W) for 30 minutes to enhance materials mixing. The mixture was filtrated via a filtration membrane with a pore size of 0.2 μm (cellulose acetate, Advantec) under positive pressure. Randomly dispersed 2H-MoS₂/CNT composite papers with a thickness of ~10 μm were washed thoroughly with distilled water to remove the dispersant and the exfoliant. All 2H-MoS₂/CNT composite papers were dried at 200 °C under vacuum for 1 h to evaporate the moisture, residual dispersant and the exfoliant, producing a final 2H-MoS₂/CNT composite papers with a electrical conductivity of ~600 S/cm.

Characterization. The exfoliated 2H-MoS₂ sheets were deposited by dip coating onto a freshly mica or Si substrate for Raman, PL, AFM and XPS studies. Raman spectra were recorded using a multipurpose spectrometer (iHR550, Horiba Jobin Yvon) with a 532 nm excitation laser source in air under ambient conditions, the power of the laser was set below 100 mW, the spot-size of the laser was approximately 5 μm, and the peak of Si at 520.7 cm⁻¹ was used for calibration. The PL spectrum was measured using a PL spectrophotometer (Hitachi F-4500, Japan). The ultraviolet-visible (UV-vis) absorbance spectra were recorded on a Unicam UV-300 UV-vis spectrophotometer using quartz cuvettes. The XPS measurements were carried out by using an Thermo K-Alpha (VGS) with Al Kα X-ray (1486.6 eV) as radiation source. The binding energies were calibrated with Au 4f_{7/2} at 84.0 eV. The morphology and structure of the exfoliated 2H-MoS₂ sheets were investigated using TEM (JEOL JEM-2100) and HRTEM (Hitachi H-7100) with the exfoliated 2H-MoS₂ sheets directly transferred onto a formvar-coated or lacey-coated copper grid. A tapping mode atomic force microscope (TM-AFM; Innova/Bruker, Santa Barbara, CA) was used to characterize the thickness of the exfoliated 2H-MoS₂ sheets. The analyses of sample weight loss were conducted using a TGA instrument (Q500, TA instrument). Electrochemical studies were measured using a CHI 7279E (CH instrument Corp.). The electrical contacts for the 2H-MoS₂/CNT paper were connected using copper alligator clip. The MoS₂/CNT paper electrodes of 1 cm × 0.5 cm were tested in 0.5 M Na₂SO₄ solution using a typical three-electrode electrochemical system, with a Ag/AgCl electrode as the reference electrode and a Pt wire as the counter electrode. Cyclic voltammetry data were recorded in between 0 V and 0.8 V vs. NHE with scan rate ranging from 1 mV/s up to 300 mV/s. The electrical conductivity of the 2H-MoS₂/CNT papers was recorded using the four-point probe method with a probe diameter of 80 μm and a distance of 1.6 mm between two adjacent probes. Measurements were carried out using a KeithLink probe station in order to provide current between -5 mA to 5 mA. Each sheet of 2H-MoS₂/CNT paper was cut into 5 cm × 5 cm squares for the electrical measurements.

References

- Novoselov, K. S. *et al.* Electric Field Effect in Atomically Thin Carbon Films. *Science* **306**, 666–669 (2004).
- Schwierz, F. Graphene Transistors: Status, Prospects, and Problems. *Proc. IEEE* **101**, 1567–1584 (2013).
- Novoselov, K. S. *et al.* Two-Dimensional Atomic Crystals. *Proc. Natl. Acad. Sci. USA* **102**, 10451–10453 (2005).
- Das, S. *et al.* Beyond Graphene: Progress in Novel Two-Dimensional Materials and van der Waals Solids. *Annu. Rev. Mater. Res.* **45**, 20.21–20.27 (2015).
- Butler, S. Z. *et al.* Progress, Challenges, and Opportunities in Two-Dimensional Materials Beyond Graphene. *ACS Nano* **7**, 2898–2926 (2013).
- Raccichini, R., Varzi, A., Passerini, S. & Scrosati, B. The Role of Graphene for Electrochemical Energy Storage. *Nat. Mater.* **14**, 271–279 (2015).
- Tour, J. M. Scaling up Exfoliation. *Nat. Mater.* **13**, 545–546 (2014).
- Zhou, K.-G. *et al.* A Mixed-Solvent Strategy for Efficient Exfoliation of Inorganic Graphene Analogues. *Angew. Chem. Int. Ed.* **50**, 10839–10842 (2011).
- Nicolosi, V. *et al.* Liquid Exfoliation of Layered Materials. *Science* **340**, 1226419 (2013).
- O'Neill, A., Khan, U. & Coleman, J. N. Preparation of High Concentration Dispersions of Exfoliated MoS₂ with Increased Flake Size. *Chem. Mater.* **24**, 2414–2421 (2012).
- Coleman, J. N. *et al.* Two-Dimensional Nanosheets Produced by Liquid Exfoliation of Layered Materials. *Science* **331**, 568–571 (2011).
- Yao, Y. *et al.* High-Concentration Aqueous Dispersions of MoS₂. *Adv. Funct. Mater.* **23**, 3577–3583 (2013).
- Lotya, M. *et al.* Liquid Phase Production of Graphene by Exfoliation of Graphite in Surfactant/Water Solutions. *J. Am. Chem. Soc.* **131**, 3611–3620 (2009).
- Py, M. A. & Haering, R. R. Structural Destabilization Induced by Lithium Intercalation in MoS₂ and Related Compounds. *Can. J. Phys.* **61**, 76–84 (1983).
- Joensen, P., Frindt, R. F. & Morrison, S. R. Single-Layer MoS₂. *Mater. Res. Bull.* **21**, 457–461 (1986).
- Eda, G. *et al.* Photoluminescence from Chemically Exfoliated MoS₂. *Nano Lett.* **11**, 5111–5116 (2011).
- Zheng, J. *et al.* High Yield Exfoliation of Two-Dimensional Chalcogenides using Sodium Naphthalenide. *Nat. Commun.* **5**, 3995 (2014).
- Wang, Q. H. *et al.* Electronics and Optoelectronics of Two-Dimensional Transition Metal Dichalcogenides. *Nat. Nanotechnol.* **7**, 699–712 (2012).
- Chhowalla, M. *et al.* The Chemistry of Two-Dimensional Layered Transition Metal Dichalcogenide Nanosheets. *Nat. Chem.* **5**, 263–275 (2013).
- Zeng, Z. *et al.* Single-Layer Semiconducting Nanosheets: High-Yield Preparation and Device Fabrication. *Angew. Chem. Int. Ed.* **50**, 11093–11097 (2011).
- Liu, N. *et al.* Large-Area Atomically Thin MoS₂ Nanosheets Prepared Using Electrochemical Exfoliation. *ACS Nano* **8**, 6902–6910 (2014).
- Smith, R. J. *et al.* Large-Scale Exfoliation of Inorganic Layered Compounds in Aqueous Surfactant Solutions. *Adv. Mater.* **23**, 3944–3948 (2011).
- May, P., Khan, U., Hughes, J. M. & Coleman, J. N. Role of Solubility Parameters in Understanding the Steric Stabilization of Exfoliated Two-Dimensional Nanosheets by Adsorbed Polymers. *J. Phy. Chem. C* **116**, 11393–11400 (2012).
- Ciesielski, A. & Samori, P. Graphene via Sonication Assisted Liquid-Phase Exfoliation. *Chem. Soc. Rev.* **43**, 381–398 (2014).
- Chen, I.-W. P., Jhou, S.-H. S. & Chen, Y.-W. Preparation of High-Quality Graphene Sheets and Their Applications in Highly Conductive Papers and a High-Performance Electromechanical Actuator. *J. Mater. Chem. C* **1**, 5970–5975 (2013).
- Chen, I.-W. P., Huang, C.-Y., Jhou, S.-H. S. & Zhang, Y.-W. Exfoliation and Performance Properties of Non-Oxidized Graphene in Water. *Sci. Rep.* **4**, 3928 (2014).
- Liang, Y. *et al.* Rechargeable Mg Batteries with Graphene-like MoS₂ Cathode and Ultrasmall Mg Nanoparticle Anode. *Adv. Mater.* **23**, 640–643 (2011).
- Kim, C. *et al.* Performances of Liquid-Exfoliated Transition Metal Dichalcogenides as Hole Injection Layers in Organic Light-Emitting Diodes. *Adv. Funct. Mater.* **25**, 4512–4519 (2015).
- Anbazhagan, R., Wang, H.-J., Tsai, H.-C. & Jeng, R.-J. Highly Concentrated MoS₂ Nanosheets in Water Achieved by Thioglycolic Acid as Stabilizer and Used as Biomarkers. *Rsc. Adv.* **4**, 42936–42941 (2014).
- Li, Y. *et al.* Nanocellulose as Green Dispersant for Two-Dimensional Energy materials. *Nano Energy* **13**, 346–354 (2015).
- Chow, P. K. *et al.* Wetting of Mono and Few-Layered WS₂ and MoS₂ Films Supported on Si/SiO₂ Substrates. *ACS Nano* **9**, 3023–3031 (2015).

32. Mi, H., Jiang, Z. & Kong, J. Hydrophobic Poly (ionic liquid) for Highly Effective Separation of Methyl Blue and Chromium Ions from Water. *Polymer* **5**, 1203–1214 (2013).
33. Lee, Y.-H. *et al.* Synthesis of Large-Area MoS₂ Atomic Layers with Chemical Vapor Deposition. *Adv. Mater.* **24**, 2320–2325 (2012).
34. Li, J. *et al.* Inkjet Printing of MoS₂. *Adv. Funct. Mater.* **24**, 6524–6531 (2014).
35. Voiry, D. *et al.* Covalent Functionalization of Monolayered Transition Metal Dichalcogenides by Phase Engineering. *Nat. Chem.* **7**, 45–49 (2015).
36. Lee, C. *et al.* Anomalous Lattice Vibrations of Single and Few-Layer MoS₂. *ACS Nano* **5**, 2695–2700 (2010).
37. Imanishi, N., Toyoda, M., Takeda, Y. & Yamamoto, O. Study on Lithium Intercalation into MoS₂. *Solid State Ionics* **58**, 333–338 (1992).
38. Zhu, Y. *et al.* Graphene and Graphene Oxide: Synthesis, Properties, and Applications. *Adv. Mater.* **22**, 3906–3924 (2010).
39. Bae, J. *et al.* Single-Fiber-Based Hybridization of Energy Converters and Storage Units using Graphene as Electrodes. *Adv. Mater.* **23**, 3446–3449 (2011).
40. Sun, G. *et al.* Hybrid Fibers Made of Molybdenum Disulfide, Reduced Graphene Oxide, and Multi-Walled Carbon Nanotubes for Solid-State, Flexible, Asymmetric Supercapacitors. *Angew. Chem. Int. Ed.* **54**, 4651–4656 (2015).
41. Sun, G. *et al.* Fabrication of Ultralong Hybrid Microfibers from Nanosheets of Reduced Graphene Oxide and Transition-Metal Dichalcogenides and their Application as Supercapacitors. *Angew. Chem. Int. Ed.* **53**, 12576–12580 (2014).
42. Chmiola, J. *et al.* Monolithic Carbide-Derived Carbon Films for Micro-Supercapacitors. *Science* **328**, 480–483 (2010).
43. Cao, L. *et al.* Direct Laser-Patterned Micro-Supercapacitors from Paintable MoS₂ Films. *Small* **9**, 2905–2910 (2013).
44. Yang, S. *et al.* Bottom-up Approach toward Single-Crystalline VO₂-Graphene Ribbons as Cathodes for Ultrafast Lithium Storage. *Nano Lett.* **13**, 1596–1601 (2013).
45. Chang, K. & Chen, W. L.-Cysteine-Assisted Synthesis of Layered MoS₂/Graphene Composites with Excellent Electrochemical Performances for Lithium Ion Batteries. *ACS Nano* **5**, 4720–4728 (2011).

Acknowledgements

The authors gratefully acknowledge the Ministry of Science and Technology (MOST), Taiwan (103-2113-M-143-003-MY2) for financial and research support. Thanks to Professor C.-h. Chen (NTU) for the use of the equipment and to Ms. S.-J. Ji, C.-Y. Chien and S. W. Hsu of Precious Instrument Center (NTU) for the assistance in SEM, TEM and TGA experiments.

Author Contributions

I.-W.P.C. designed the exfoliation experiments. Y.X.C. and C.W.W. performed the dispersion experiments. I.-W.P.C. wrote the paper and took the photograph of the Fig. S1. All the authors discussed the data and commented on the manuscript. All authors reviewed the manuscript.

Additional Information

Supplementary information accompanies this paper at <http://www.nature.com/srep>

Competing financial interests: The authors declare no competing financial interests.

How to cite this article: Chen, Y.-X. *et al.* Large-Scale Production of Large-Size Atomically Thin Semiconducting Molybdenum Dichalcogenide Sheets in Water and Its Application for Supercapacitor. *Sci. Rep.* **6**, 26660; doi: 10.1038/srep26660 (2016).



This work is licensed under a Creative Commons Attribution 4.0 International License. The images or other third party material in this article are included in the article's Creative Commons license, unless indicated otherwise in the credit line; if the material is not included under the Creative Commons license, users will need to obtain permission from the license holder to reproduce the material. To view a copy of this license, visit <http://creativecommons.org/licenses/by/4.0/>